

EBNA1-specific luminescent small molecules for the imaging and inhibition of latent EBV-infected tumor cells†

Cite this: *Chem. Commun.*, 2014, 50, 6517

Received 3rd March 2014,
Accepted 28th March 2014

DOI: 10.1039/c4cc01589d

www.rsc.org/chemcomm

An EBNA1-specific small molecule (JLP₂) has been synthesised. As a strong binder and dimerization inhibitor of EBNA1 *in vitro*, JLP₂ may be used as a selective luminescent agent for the imaging and inhibition of latent EBV-infected cancer cells.

The Epstein–Barr virus (EBV) is etiologically implicated in several lymphoid and epithelial malignancies, substantially contributing to the growth of a diversity of lymphomas and carcinomas. Identifying the presence of EBV in the cells of EBV-associated cancers can, therefore, provide an overarching target for specific therapies.¹ Although current treatments for EBV-associated carcinomas, such as radiotherapy and chemotherapy, have long been adopted, the former is inadequate at killing advanced metastatic tumors or preventing their recurrence, while the latter is still under development.^{2,3} In fact, a dimeric viral oncoprotein, Epstein–Barr nuclear antigen (EBNA1), is found to be responsible for the development of EBV-related malignancies and the maintenance of the EBV episome. Given that the carcinogenesis of EBV-associated carcinomas is symbiotically connected with EBV infection, and that EBNA1 can function (*e.g.* replicate, bind DNA and transactivate) only upon dimerization (formation of the active form), we hypothesize that a fluorescent probe consisting of a chromophore and an EBNA1-specific molecule, which hampers the formation of the dimer, can be used for the imaging and

inhibition of latent EBV-infected cells (Fig. 1a). This study will provide a novel strategy for interfering with the growth of EBV-associated tumors.^{1–7} Recently, two groups of novel EBNA1 inhibitors, known as Eik1 and peptide inhibitors, have been introduced. Eik1, developed under a high-throughput screening, is a small molecule which can effectively inhibit the

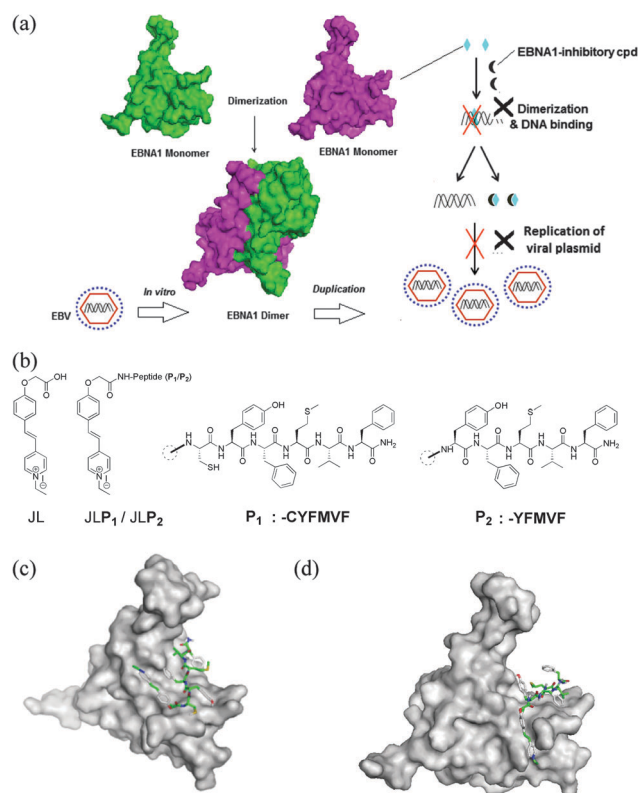


Fig. 1 (a) The schematic model shows the inhibition of the processes of EBV infection of the host cell and virus reproduction by our compounds; (b) the chemical structures of EBNA1 specific peptides (**P₁** and **P₂**) conjugated with water soluble luminescent moieties; (c) and (d) the binding fitting model, obtained *via* molecular modeling, for the comparison of interactions between JLP₁/JLP₂ and EBNA1.

^a Department of Chemistry, Hong Kong Baptist University, Kowloon Tong, Hong Kong SAR. E-mail: kh Wong@hkbu.edu.hk; Tel: +852-34112370

^b Department of Biology, Hong Kong Baptist University, Kowloon Tong, Hong Kong SAR. E-mail: nkmak@hkbu.edu.hk; Tel: +852-34117059

^c Institute of Research and Continuing Education, Hong Kong Baptist University, Shenzhen, P. R. China

^d Department of Biology and Chemistry, City University of Hong Kong, Kowloon Tong, Hong Kong SAR

^e Department of Anatomy, The University of Hong Kong, Hong Kong SAR

† Electronic supplementary information (ESI) available: Experimental information for the synthesis and purification of EBNA1, MTT assays and *in vitro* imaging; high resolution mass spectra of **P₁**, **P₂**, **JLP₁** and **JLP₂**; NMR spectra of intermediates, ligands of **JLP₁** and **JLP₂**; emission spectra of **JLP₁** with the addition of various amounts of EBNA1. See DOI: 10.1039/c4cc01589d

dimerization *via* association with amino acids 459–607 of the dimerization domain of EBNA1, whilst the peptidic counterpart functions similarly in the region of 560–574.^{8,9} In *in vitro* cell line reporter studies, both inhibitors worked well in the EBNA1-dependent, OriP-enhanced transcription of SEAP (secreted alkaline phosphatase). However, their activities in EBV-positive tumor cells have not been reported, and these inhibitors cannot be visualized by confocal microscopy. Additionally, the poor solubility of the published peptides (*e.g.* p85) hinders their application.^{9,10}

There are many validated anticancer drug targets, such as cyclins, polo-like kinase (Plk) or even EBV, and recent research has reported that these targets can be inhibited by various tailor-made peptides. However, the major challenges of using peptides as anti-tumor agents *in vitro/in vivo* lie in achieving cellular internalization, their sensitivity towards enzymes *in vivo* and the difficulty of monitoring *via* indirect screening. It is widely acknowledged that proteins/peptides presenting cationic surfaces can permeate the cell membranes of eukaryotic and endogenous cells. The attachment of luminescent cargos (*i.e.* organic molecules/nanomaterial/metal complexes) can provide real time monitoring of these peptides' functions and improve their cell permeability and solubility. Herein, we report our newly developed EBNA1-specific dual bioprobe (JLP₂ - Fig. 1b), which conjugates with EBNA1-specific peptides. The design rationale is based on molecular computation (*vide infra*) and synthetic simplicity. Experiment-wise, JLP₁ and a well-known mitochondrial marker, chromophore JL,¹¹ served as the control. As expected, JLP₂ illustrated selective and responsive emission enhancement upon specific binding with EBNA1, both under aqueous conditions and *in vitro*, with EBV-infected tumor cells. The IC₅₀ of JLP₂ in latent EBV-infected tumor cells was much higher than in non-EBV-infected tumor cells. In addition, we calculated the binding affinities of Eik1, JLP₁ and JLP₂ for EBNA1, *via* molecular docking, and

compared the interactions.¹² (Fig. 1b and c - JLP₁ with EBNA1, -7.6 kcal mol⁻¹ and JLP₂ with EBNA1, -9.0 kcal mol⁻¹.) The result shows that JLP₂ does bind EBNA1 more strongly than JLP₁ and Eik1 (Eik1 = -6.9 kcal mol⁻¹) (Fig. 1c and d). Based on comprehensive studies (molecular docking, spectroscopy, MBS cross-linked SDS-PAGE assay and *in vitro* imaging), JLP₂ shows potential as a specific dual bioprobe that can trace EBNA1 *in vitro* for both the imaging and inhibition of latent EBV-infected tumor cells. Known EBNA1 specific compounds, namely Eik1 and the aforementioned peptides, are not visualized in cells.

JLP₁ and JLP₂ were purified by HPLC and characterized by NMR and high resolution mass spectroscopy (ESI⁺). The absorption and emission bands of JLP₁ and JLP₂ are 30 nm red shifted compared with JL (due to the conjugation of peptides P₁/P₂ to JL). For JLP₁ and JLP₂, the absorption and excitation bands are very similar at 375 nm (JLP₁) and 390 nm (JLP₂) in aqueous solution (Fig. 2). The emissions of both JLP₁ and JLP₂ are green ($\lambda_{em} = \sim 560$ nm, $\lambda_{ex} = 400$ nm, Fig. 2) In comparison with the EBNA1-specific small molecules/peptides in the literature, our compounds are fluorescent, meaning that the binding of EBNA1 *in situ/in vitro*, or their cellular uptake, can be evaluated directly by fluorescence detection, *i.e.* flow cytometry and fluorescence microscopy. The general

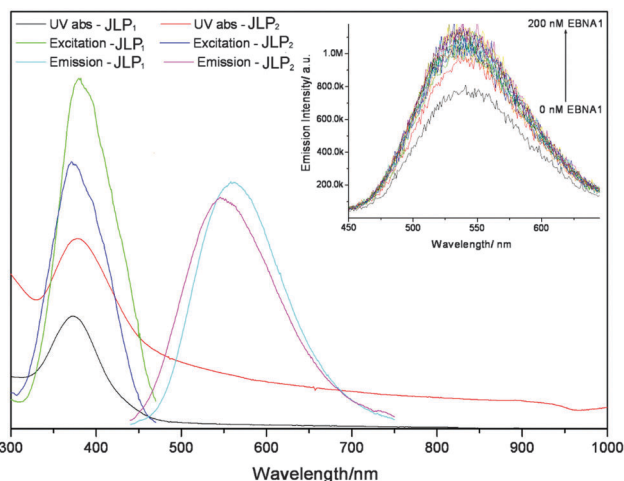


Fig. 2 The UV absorption, excitation (JLP₁ - $\lambda_{em} = 545$ nm and $\lambda_{em} = 560$ nm) and emission spectra ($\lambda_{ex} = 405$ nm) of JLP₁ and JLP₂ in aqueous solution. Inset: the emission enhancement of JLP₂ upon the addition of the 200 nM EBNA1.

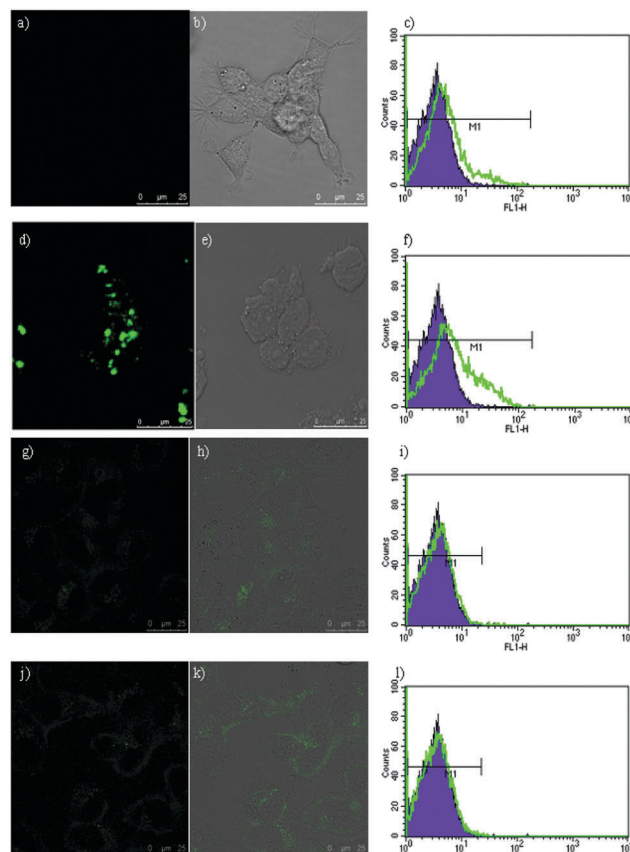


Fig. 3 The confocal images and cellular uptake (by flow cytometry) of JLP₁ and JLP₂ in latent EBV-infected nasopharyngeal carcinoma C666-1 cells (a–c - JLP₁; d–f - JLP₂) and non-latent EBV-infected human cervical carcinoma HeLa cells (g–i - JLP₁; j–l - JLP₂).

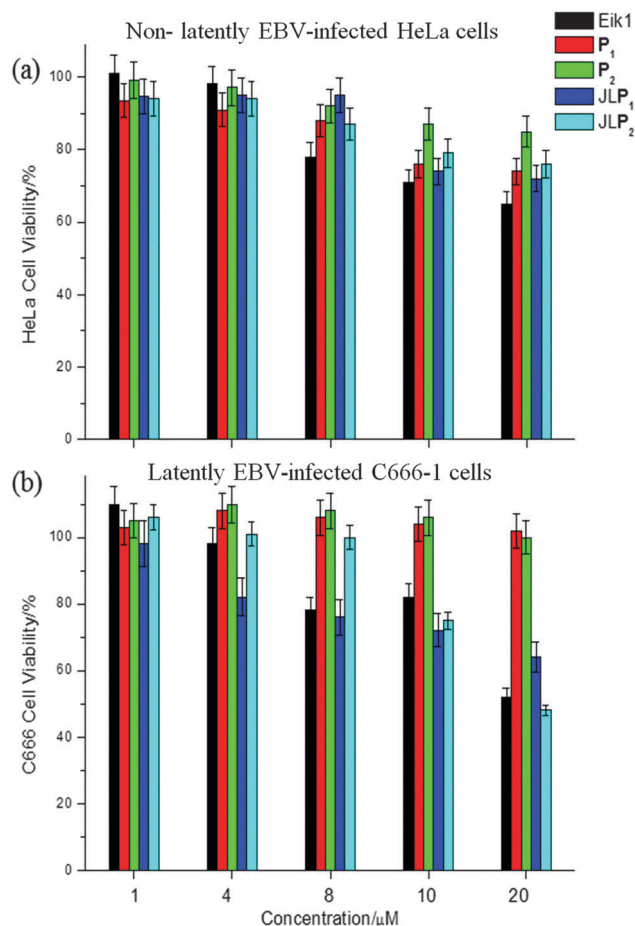


Fig. 4 The inhibitory activities, measured by cell viability, of two EBNA1 specific peptides (**P₁** and **P₂**), two small molecules (**JLP₁** and **JLP₂**) and Eik1 (control) on (a) non-latent EBV-infected human cervical carcinoma HeLa cells and (b) latent EBV-infected nasopharyngeal carcinoma C666-1 cells.

photophysical properties of **JLP₁** and **JLP₂** are similar, as only one amino acid in their structures is different; however, the *in situ* and *in vitro* behaviours of **JLP₁** and **JLP₂** are completely distinct. For instance, after the addition of EBNA1 into the aqueous solutions of **JLP₁** and **JLP₂**, emission enhancement could be detected only for **JLP₂**, more or less 1.5-fold upon the addition of 200 nM EBNA1 (inset of Fig. 2), whereas, for **JLP₁**, the emission intensity was slightly diminished with the same dose of EBNA1 in water (Fig. S14, ESI[†]). Aside from this, we had also confirmed the specific binding of **JLP₂** to EBNA1 by MBS (3-maleimidobenzoyl *N*-hydroxysuccinimide) cross-linked SDS-PAGE assay. MBS can form covalent cross-linkages with dimerized EBNA1 proteins, which can be separated using SDS-PAGE. That is, EBNA1, disrupted by the compound in the assay, can no longer exist as a dimer. In Fig. S16 (ESI[†]) (black box), it can be seen that only **JLP₂** obviously decreased the amount of dimeric EBNA1.

In addition, the cellular uptake of **JLP₁** differs from that of **JLP₂**. **JLP₁** and **JLP₂** (10 μM) were tested in latent EBV-infected nasopharyngeal carcinoma C666-1 cells for 12 hours. The uptake of **JLP₂** could be observed more apparently: the confocal images from the C666-1 cells in the presence of **JLP₁** and **JLP₂** have been related to the findings from the flow cytometry uptake studies (Fig. 3). No emission can be obtained from **JLP₁** in the C666-1 cells and only **JLP₂** displays impressive emission in the latent EBV-infected nasopharyngeal carcinoma C666-1 cells in the same experiment.

In the cytotoxicity experiment (**JLP₁** and **JLP₂** in EBV/non-EBV infected tumor cells, and Eik1 as the control), **JLP₂** demonstrated smaller IC₅₀ values in EBV infected cancer cells (C666-1, ~IC₅₀ = 20 μM, similar to the Eik1) than in non-EBV infected cancer cells (HeLa, ~IC₅₀ = 1 mM). On the other hand, **JLP₁**, **P₁** and **P₂** demonstrated similar IC₅₀ values with HeLa and C666-1 cells under the same experimental conditions. Peptides **P₁** and **P₂** are not cell permeable and alone are not effective in preventing the growth of carcinoma cells, and so served as the control experiments in the MTT assays (Fig. 4).

A specific and selective agent for both the imaging and targeting of this virus-associated tumor is not currently available in the literature. In this regard, we have synthesised a dual-function fluorescent probe (**JLP₂**) of verified applicability for the simultaneous imaging and control of the growth of a tumor latently infected with EBV (*e.g.* nasopharyngeal carcinoma), on account of the probe's underlying mechanism of specifically preventing the dimerization of EBNA1.

This work was funded by grants from The Hong Kong Research Grants Council (HKBU 203013), City University of Hong Kong, and Hong Kong Baptist University (FRG 2/12-13/069).

Notes and references

- H. K. Koon, P. S. Chan, R. N. S. Wong, Z. G. Wu, M. L. Lung, C. K. Chang and N. K. Mak, *J. Cell. Biochem.*, 2009, **108**, 1356.
- L. S. Young and A. B. Rickinson, *Nat. Rev. Cancer*, 2004, **4**, 757; K. C. Chan, C. M. Ting, P. S. Chan, M. C. Lo, K. W. Lo, J. E. Curry, T. Smyth, A. W. M. Lee, W. T. Ng, G. S. W. Tsao, R. N. S. Wong, M. L. Lung and N. K. Mak, *Mol. Cancer*, 2013, **12**, 128.
- G. Kennedy and B. Sugden, *Mol. Cell. Biol.*, 2003, **23**, 6906.
- A. T. C. Chan, V. Grégoire, J.-L. Lefebvre, L. Licitra and E. Felip, *Ann. Oncol.*, 2010, **21**, 187.
- L. Frappier, *Scientifica*, 2012, **2012**, 438204.
- D. W. Smith and B. Sugden, *Viruses*, 2013, **5**, 226.
- S. J. Duellman, K. L. Thompson, J. J. Coon and R. R. Burgess, *J. Gen. Virol.*, 2009, **90**, 2251.
- N. Li, S. Thompson, D. C. Schultz, W. Zhu, H. Jiang, C. Luo and P. M. Lieberman, *PLoS One*, 2010, **5**, e10126.
- S. Y. Kim, K. A. Song, E. Kieff and M. S. Kang, *Biochem. Biophys. Res. Commun.*, 2012, **424**, 251.
- M. Kenji, Y.-S. Naoko, O. Chikashi, T. Toshiki and M. Hisao, *J. Biol. Chem.*, 2012, **287**(28), 23977.
- G. R. Rosania, J. W. Lee, L. Ding, H.-S. Yoon and Y.-T. Chang, *J. Am. Chem. Soc.*, 2003, **125**, 1130.
- O. Trott and A. J. Olson, *J. Comput. Chem.*, 2010, **31**, 455.